Analysis of

Comparing Aerodynamic Efficiency in Birds and Bats Suggests Better Flight Performance in Birds

Paper Authors: Florian T. Muijres, L. Christoffer Johansson, Melissa S. Bowlin, York Winter, Anders Hendenström
Published in PLoS ONE, May 2012

Analysis by Rónán Gissler
May 4th, 2021

Summary:

The purpose of the research discussed in this paper was to compare the flight performance between birds and bats experimentally. The two metrics used to measure flight performance were span efficiency and lift-to-drag ratio, metrics for efficiency of lift generation and mechanical energetic flight efficiency respectively. In order to derive these metrics, the researchers estimated aerodynamic forces on the animals by applying basic vortex theory to the wake structures produced behind the animals as they flew. The authors summed the forces produced by four key vortex structures in the animal's wake to determine the overall aerodynamic forces acting on the animal. Then the lift-to-drag ratio is simply the ratio of the two aerodynamic forces, while the span efficiency was calculated using a modified actuator disk model developed in their previous research. The wake structures were recorded using time-resolved stereo Particle Image Velocimetry (PIV) measurements as the test animals flew in a low turbulence wind tunnel steadily against the wind to maintain proximity to a feeder. Additionally, high-speed cameras were used to simultaneously capture the wingbeat kinematics of the animals. Two species of both bats and birds were selected which fly in similar fluid regimes ($Re \sim 10^4$), including three pied flycatchers, one blackcap, two Pallas' long-tongued bats, and two lesser long-nosed bats.

Both birds and bats produced vortices at the tip and root of their wings, with root vortices lasting longer throughout the wingbeat cycle in bats. In addition to these vortex structures, birds produced tail vortices while bats produced reversed vortex loops behind each wing. The authors' attributed the formation of these unique vortex structures between birds and bats to different wingbeat upstroke action. Bats move their wings upwards at a negative angle-of-attack generating reversed vortex loops, in turn producing positive thrust and negative lift—hence the "reversed". On the other hand, birds make their wings inactive during the latter part of the upstroke by retracting them and spreading the primary wing feathers resulting in dominance of body lift and the generation of tail vortices. As a result of these different wake dynamics, the lift-to-drag ratio and span efficiency during one wingbeat were significantly higher for the birds than the bats. Nonetheless, previous research cited by the authors showed that the observed wingbeat kinematics, in particular the negative lift during upstroke in bats and positive lift during upstroke in birds, was energetically optimal for wings at the lift-to-drag ratio of each flier. Instead of differences in wingbeat kinematics, the authors accredited the lower body lift produced by bats—evidenced by reduced downwash in the wake—to the observed lower flight efficiency in bats. The authors' hypothesized the lower body lift in bats may be a result of a less streamlined body morphology, in particular protruding ears used for echolocation. After reviewing the different ecology of the species studied, including migration and feeding habits, the researchers did not identify any clear ecological explanation for the difference in flight efficiency between birds and bats. Therefore, the researchers concluded that their results suggested evolution had optimized performance for the respective conditions of birds and bats, but that the maximum performance was limited by phylogenetic constraints on wing and body morphology.

Turbulence-Studying Technique:

To study the vortex structures produced in the wake of the fliers, the researchers used time-resolved stereo Particle Image Velocimetry (PIV) measurements as the test animals flew in a low turbulence wind tunnel steadily against the wind to maintain proximity to a feeder. The wind tunnel, located at Lund University, was filled with a thin fog such that fluid particles could be observed through PIV (Hedenström et al., 2009). A number of different flight speeds ranging 2-9 m/s were tested by setting the speed of air moving through the wind tunnel, but not all animals were tested at the same speeds. The stereo PIV system consisted of a pair of high-speed (200 Hz) cameras located downstream of the flier, capturing the wake produced behind the flier as it flew steadily against the wind in front of a stationary laser sheet perpendicular to the streamwise direction (see Appendix Figure 1). Simultaneously, two high-speed (250 Hz) cameras were used to record the wingbeat kinematics of the flier.

The reference frame used throughout the analysis is as follows: positive displacement {x} and velocity {u} in the downstream direction, positive displacement {y} and velocity {v} to the right of the flier, and positive displacement {z} and velocity {w} directed opposite gravitational acceleration. PIV frames were analyzed over the course of one wingbeat and each frame was assigned a frame number, dimensionless time, and streamwise position. The frame number was defined as n=[1,N], where n=1 is the start of the downstroke and n=N is the end of the upstroke. The dimensionless time was defined as τ=[0,1], where τ=0 is the start of the downstroke and τ=1 is the end of the upstroke (τ=t/Π where Π is the wingbeat period). The streamwise position was defined as x=[0,λ] where λ is the wingbeat wavelength which equals the wind speed of the tunnel divided by the wingbeat frequency ($\lambda = \frac{U}{f}$).

Using the commercially available DaVis image analysis software, each PIV frame was processed to return a 3D velocity vector {u, v, w} for each node in the frame {y, z}. Taking the curl of the 3D velocity vector at each node produces a 3D vorticity field. Within each frame, vortex structures were identified as "compact, contiguous patches of high vorticity magnitude" (Muijres et al., 2011). The vortex structures identified include tip vortices, root vortices, tail vortices, and reversed vortex loops. These vortex structures were not necessarily present for all fliers or throughout the entire wingbeat cycle. The position {x, y, z} and circulation of each vortex structure was then analyzed in Matlab. Piecing together multiple PIV frames across the time of a single wingbeat as the wake structures move downstream, the wake topology of the flier can be represented using vorticity isosurfaces.

Using the circulation and span of each vortex structure, the aerodynamic forces were calculated using basic vortex theory. The key principle behind this approach lies in conservation of momentum. The aerodynamic force acting on the flier as it moves its wings is the result of the wings generating momentum flow in the air, shedding off the flier in the form of vortex structures (Ellington, 1984). The expression for normalized (divided by animal weight) aerodynamic lift resulting from each vortex structure is as follows:

$$L^*(\tau) = [\rho\ U\ b_w(\tau)\ \Gamma(\tau)] / W$$

ρ: Air Density
U: Tunnel Air Speed (equivalent to animal flight speed)
$b_w(\tau)$: Wake Span (spanwise distance between paired vortex structures from each wing) (see Appendix Figure 2)
$\Gamma(\tau)$: Vortex Circulation (integral of vorticity over vortex area)
W: Animal Weight

This expression for the lift force appears to follow a similar form to the typical lift equation using a lift coefficient equal to $C_L = 2 * \Gamma(\tau)/U\bar{c}$ where $\bar{c}$is the mean chord length (Muijres et al., 2008). Assuming the aerodynamic force resulting from each vortex structure acts perpendicular to the instantaneous axis of the vortex tube, the normalized aerodynamic thrust resulting from each vortex structure is then determined using trigonometry as follows:

$$T^*(\tau) = L^*(\tau) \tan(\bar{\gamma}(\tau))$$

$\bar{\gamma}(\tau)$: Mean Streamwise Vortex System Angle (Mean angle between stream and vortex tube. Mean calculation is different for different vortex structures)(see Appendix Figure 2)

Since the fliers are in nearly steady flight as they fly against the wind to remain next to the feeder, the authors' assumed that the thrust produced by the flier directly counters the drag and thus the two would be equal in magnitude. Expressions for total normalized lift and drag as a function of dimensionless time are determined by summing the contribution from each vortex structure. Then for each speed and species combination, these temporal normalized lift and drag expressions are averaged across all recorded wingbeat trials using smoothing splines resulting in an average temporal normalized lift $\overline{L^*}(\tau)$ and average temporal normalized drag $\overline{D^*}(\tau)$. Finally, to determine the mean lift and drag across one wingbeat for each species and speed combination, the average temporal normalized lift and drag are integrated with respect to dimensionless time. It's worthwhile noting that the integral of a normalized function equals the mean value since the range of the function is [0,1]. Having determined the wingbeat average lift and drag forces, the wingbeat average lift-to-drag ratio can easily be determined by taking the ratio of the two aerodynamic forces.

To calculate the span efficiency requires determining the real and ideal induced power from lift production. Here the authors use a modified actuator disk model developed in their previous work to estimate the power resulting from lift production. The actuator disk model is a simplified model for force and power estimations of constantly rotating wings (Muijres et al., 2011). It was originally developed for helicopter rotors, but has since been adapted for flapping

animal flight. Again, the key principle behind this model lies in conservation of momentum. The model defines an actuator disk as an area swept by the wing configuration. For a helicopter this is easy to picture, but with flapping wings on an animal it becomes more difficult. Traditionally, the actuator disk for flapping flight was defined as a circular area with diameter equal to the wingspan, but the authors' modified the model to define the area as that bounded by the tip vortex tubes during a single wingbeat cycle. In other words, the area can be constructed by tracing between the two tip vortices across all the PIV frames over the course of one wingbeat. Having determined what the actuator disk is, the lift force on the flier is then equal in magnitude and opposite in direction to the momentum flow rate of air through the actuator disk.

The induced power from lift production is equal to the magnitude of the product of the lift force and the induced vertical velocity at the actuator disk. For the real induced power, the real induced vertical velocity distribution under the wingspan—also referenced by the authors' as the "downwash distribution"—is used. From the PIV data, this "downwash distribution" can be determined by noting the vertical velocity component at each node along the span of the body between tip vortices. For the ideal induced power, a uniform induced vertical velocity distribution is used which would generate an equivalent amount of lift. This uniform induced vertical velocity distribution can be found simply by rearranging the lift equation to solve for the velocity. Therefore, the ideal induced power represents the minimum induced power to generate the required lift. Dividing the wingbeat ideal induced power by the wingbeat real induced power produces the span efficiency for a complete wingbeat. It should be noted that the span efficiency only takes into account the induced drag—the drag resulting from the downwash behind the animal (Muijres et al., 2012). Drag produced by the body (parasite drag) and by the wing (profile drag) are not accounted for in this metric (Muijres et al., 2012). Consequentially, this metric only provides a piece of the picture in describing flight efficiency. As flight speed increases, parasitic and profile drag will also increase, making it more difficult to distinguish the flight efficiency between fliers using the span efficiency alone as a metric (Hubel et al., 2016).

Review:

The method by which the authors' employed PIV in their study of wake dynamics behind birds and bats was not clearly outlined in this paper, requiring one to review several of their previous papers to fully understand their methods. One of the key assumptions made by the authors that is of questionable validity is what one source citing this work deemed the "frozen flow assumption" (Horstmann et al., 2014). The authors' assume that, once formed, the vortex structures convect statically downstream at the wind tunnel speed. In other words, in the time between the vortex structure generation at the birds wing and the time the vortex structure then crosses the laser sheet to be imaged, the vortex structure does not deform or evolve significantly. Obviously this is an unreasonable assumption over long spans of time, so the question then becomes how long does it take the vortex structure to travel from the wing to the imaging plane. In one of their earlier papers, the authors stated "the vortex travel time from the wing tip to the imaging plane was about 0.04 s, which is $0.4–0.6T_w$, where T_w is the time for one wingbeat

cycle." (Hedenström et al., 2009) Although 0.04 seconds doesn't sound like much, that's also about half the wingbeat cycle of the flier. It seems highly likely that the vortex structures had the opportunity to experience significant deformation before reaching the imaging plane, particularly the tip and root vortices which are located close to one another on the wing and have opposite signs. As a result of this "frozen flow" assumption, error may have been introduced in the calculation of aerodynamic forces and induced power. To their credit, the authors clearly stated this assumption and also noted that any error in determining the vortex wake dynamics wasn't significant as the lift-to-weight ratios they calculated were close to one.

When calculating the aerodynamic forces, it was interesting to note that only contributions from discrete vortex structures were considered. It would seem more accurate to integrate the contributions from vorticity across the wing rather than just including the distinct patches where vorticity was strongest. However, it's difficult to imagine how this could be achieved using the method employed by the authors as many of their calculations require an understanding of a vortex with defined area and location.

The purpose of the authors' paper is, as evidenced by its title, to compare flight efficiency between birds and bats. Nonetheless, the authors also make the argument that because they observed higher flight efficiency in birds than bats, birds are thus higher performing fliers. This argument fails to take into account other important flight metrics beyond flight efficiency such as maneuverability and agility, defined as the ability to reorient the velocity vector and ability to change angular rates respectively (Ajanic et al., 2020). Since the ability to reorient the velocity vector is dependent upon the magnitude of aerodynamic forces acting on the flier, fliers experiencing larger aerodynamic forces are predicted to be more maneuverable. Looking at the supplementary plots comparing normalized lift for the different fliers, it can be seen that the normalized lift is on average greater in the bats than in the birds (see Appendix Figure 3). This would indicate that the bats studied possess greater maneuverability than the birds. Other studies have also hypothesized greater maneuverability in bats as compared to birds which they have attributed to the lower wing loading in bats on average (Hedenström et al., 2015). Therefore, a more appropriate conclusion for the authors to make would have been that lower flight efficiency observed in the bats may be a tradeoff for their greater maneuverability. Generalizations about flight performance should not be made between phylogenies as performance likely varies substantially within each phylogeny dependent upon species-specific ecology.

Impact:

The work presented in the authors' paper provides aerodynamic forces and efficiency metrics for bats and birds flying at a similar fluid regime using PIV measurements from the vortex structures present in the wakes of the animals. In total, four unique vortex structures—tip vortices, root vortices, tail vortices, and reversed vortex loops—were identified in the wakes and explained by recorded wingbeat kinematics. The efficiency metrics they calculated include the familiar lift-to-drag ratio but also the span efficiency which they introduced to their field as

another relevant flight efficiency metric that should be considered. The efficiency metrics were higher in the birds than bats, suggesting higher flight efficiency in birds.

Conducting PIV experiments is prohibitively expensive if one does not already have access to a wind tunnel, high-speed PIV cameras, and laser with associated optical equipment. Nonetheless, several later studies inspired by the work in this paper conducted their own PIV experiments to challenge the conclusions presented by the authors. Crandell et al. (2015) sought to test the hypothesis that upstroke in birds produces insignificant aerodynamic forces as was stated in the authors' paper based on the kinematic data showing the birds retracting their wings and holding them inactive during the latter part of the upstroke. Crandell et al. hypothesized that birds using a wingtip-reversal upstroke as opposed to the flexed-wing upstroke used by the bird species studied in the authors' paper would result in more considerable aerodynamic forces. Through a combination of PIV, near-wake streamline measurements, and 3D kinematics imaging Crandell et al. observed significant aerodynamic forces in a bird species using the wingtip-reversal upstroke while minimal aerodynamic forces were noted in a bird species using the flexed-wing upstroke. These experiments from Crandell et al. make clear that the conclusions drawn for the few bird and bat species studied by the authors cannot be generalized to represent their whole respective phylogenies. This was reiterated by Hubel et al. (2016) who argued that the span efficiency in aerial-hunting bats may be more comparable to birds as opposed to the nectar-feeding bats studied by the authors. Hubel et al. supported this claim using PIV and kinematic imaging where they noted weak root vortices at high speeds in the aerial-hunting bats indicating significant body lift unlike the low body lift predicted for the nectar-feeding bats in the authors' paper. A study by McCracken et al. (2016) documenting natural flight speeds of a bat species known for its fast flight, also argued against the supposed underperformance of bats compared to birds by recording bat flight speed comparable to some bird species. Neither Crandell et al. or Hubel et al. calculated the span efficiency due to low resolution in their flow data.

Some higher resolution PIV studies of insects did however calculate span efficiences with which to compare against the calculated span efficiences for the bird and bat species in this paper. Henningsson et al. (2011) studied time-varying span efficiency throughout the wingbeat of desert locusts which they argued to be more informative than simply the average wingbeat span efficiency presented by the authors. Even so, they also calculated an average wingbeat span efficiency to compare against the average wingbeat span efficiencies of the birds and bats studied in this paper. Since Henningsson et al. used the traditional actuator disk model defining the actuator disk by the animal's wingspan rather than the modified actuator disk model using the area traced by the wingtip vortices as the authors had done, the comparison isn't truly representative. Regardless, they noted lower span efficiences in the desert locusts than the birds and bats studied by the authors. Later, Henningsson et al. (2013) studied the span efficiency of hawkmoths—using the same traditional actuator disk model—which they found to be lower than that in the desert locusts.

The wake structures identified in this paper also changed the discussion on wake dynamics. Previous research had primarily focused on the tip vortices and corresponding aerodynamic force contribution from these Leading Edge Vortices (LEV). Noting the substantial difference in terms of which vortex structures were present in the wakes of birds and bats, Sapir et al. (2014) cautioned against continuing to apply flight models for birds to bats. They further supported this claim through their study of how bats adjust their flight speeds to wind patterns by showing that a computer flight model for birds consistently mispredicted flight speeds for the bats. Horstmann et al. (2015), inspired by the prominence of root vortices in the wake topologies of the birds and bats studied, performed PIV measurements to study wake deformation downstream of different airfoils. They found that wake deformation was most severe behind wings with lower aspect ratios and when the distance between the wings was small. Animals that might fall under this category should accordingly be considered at high risk for measurement error due to the likelihood of significant wake deformation before the wake reaches the imaging plane. Aspect ratios of both the birds and bats tested by the authors were significantly higher than all airfoil aspect ratios tested by Horstmann et al., indicating that the test animals did not fall under this high measurement error risk category. Later research by the authors showed that an understanding of how the vortex structures are exhibited for different animals, at different speeds, and during different parts of the wingbeat cycle can be used to identify and describe import flight behaviors instead of just doing this using kinematics alone as was typical (Hedenström et al., 2015).

Furthermore, several studies explored the kinematics and morphology of birds and bats in greater detail in an attempt to explain the observed lower flight efficiency in bats (Chin et al., 2017; Busse et al., 2012). For example, Busse et al. suggested that the highly compliant wing membrane and flexible wing structure in bats—which enables them to more carefully control their wing shape and motion than other fliers—may be responsible for their lower flight efficiency.

Future Work:

Based on the analysis presented here, future work building off of this study can be carefully planned to further move forward this field of research. One possible avenue for future research would be to apply the authors' method of flight performance analysis using combined wake structure and kinematics to fliers as they exhibit landing maneuvers. Since the animals studied by the authors are flying against the wind to maintain proximity to a feeder, their study of flight is limited to steady station-holding flight. The wake structures and kinematics involved in other flight behaviors—like landing, turning or takeoff—are likely quite different. Although kinematics studies have been conducted to examine landing behaviour in flying animals, the additional information provided by the wake structures could prove useful in understanding landing behaviors in greater depth as was exemplified by the authors in their study of wake structures during steady station-holding flight. The results of such a study would provide useful insight for biologists into the landing behaviors of the test animals which could be used to further

study how ecology impacts animal behavior at the level of landing aerodynamics. Additionally, through a closer study of how animals manipulate their bodies to achieve wake dynamics that then generate aerodynamic forces directing the animals to a perch, roboticists could seek to imitate these actions to produce robots capable of perching.

Despite the potential error that arose from the distance between the animals and imaging plane due to wake deformation, a stationary imaging plane was acceptable when examining station-holding flight as the animals were positioned relatively consistently just upstream of the imaging plane. However, when studying landing maneuvers the animal must have some net velocity relative to its perch. This would lead to growing errors due to wake deformation as the animal moved further upstream of a stationary imaging plane towards its perch. Instead, the laser sheet could be projected from a moving sled using a camera to track directly behind the animal, capturing its instantaneous wake structure. This method would also allow for mitigation of any error associated with the wake structures deforming before reaching the imaging plane by minimizing the distance between the animal and imaging plane. In order to maximize the application of the results from such a study, efforts should be made to select animals spanning diverse ecologies, morphologies, and wingbeat kinematics.

Appendix:

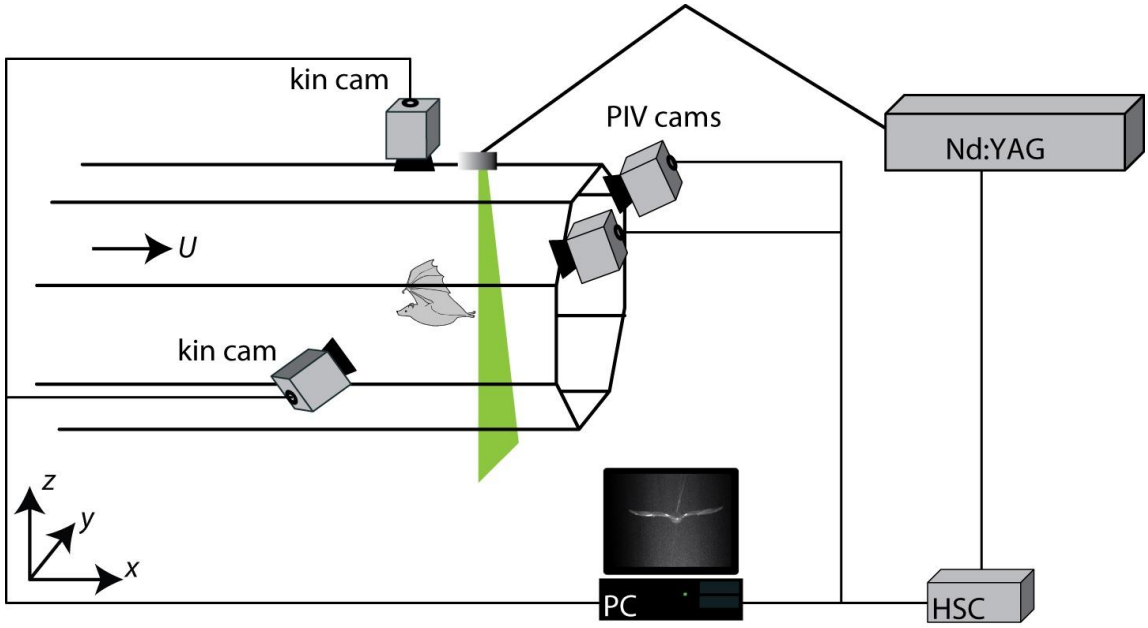

Figure 1. Experimental Setup (supplementary Figure S1 in paper)

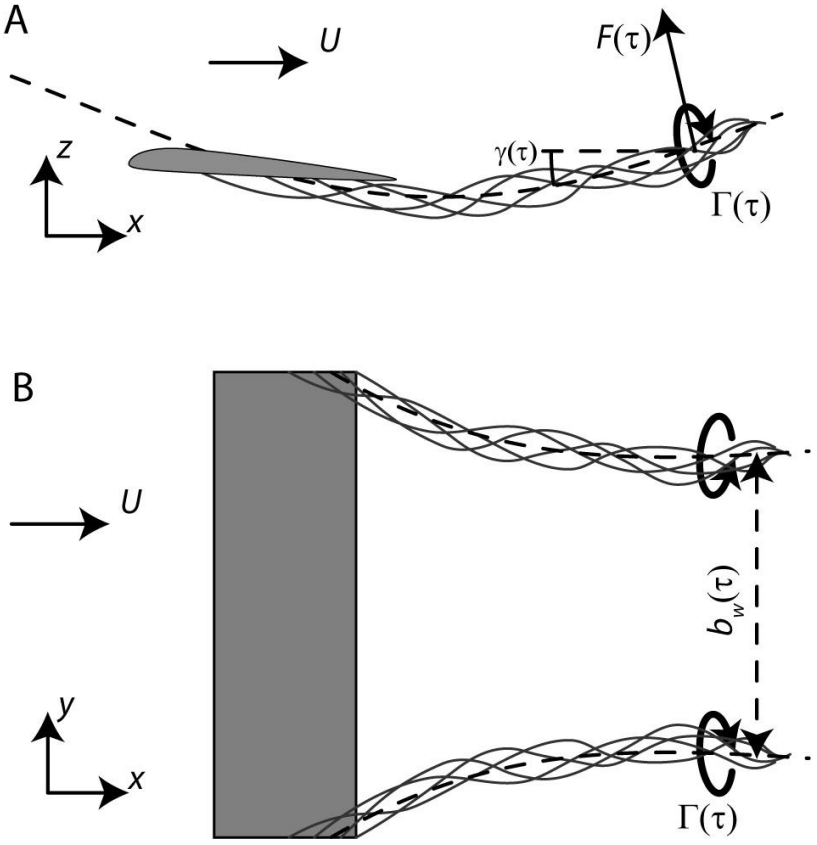

Figure 2. Tip Vortices and Time-Varying Aerodynamic Force Generated By Hypothetical Flapping Wing (supplementary Figure S2 in paper)

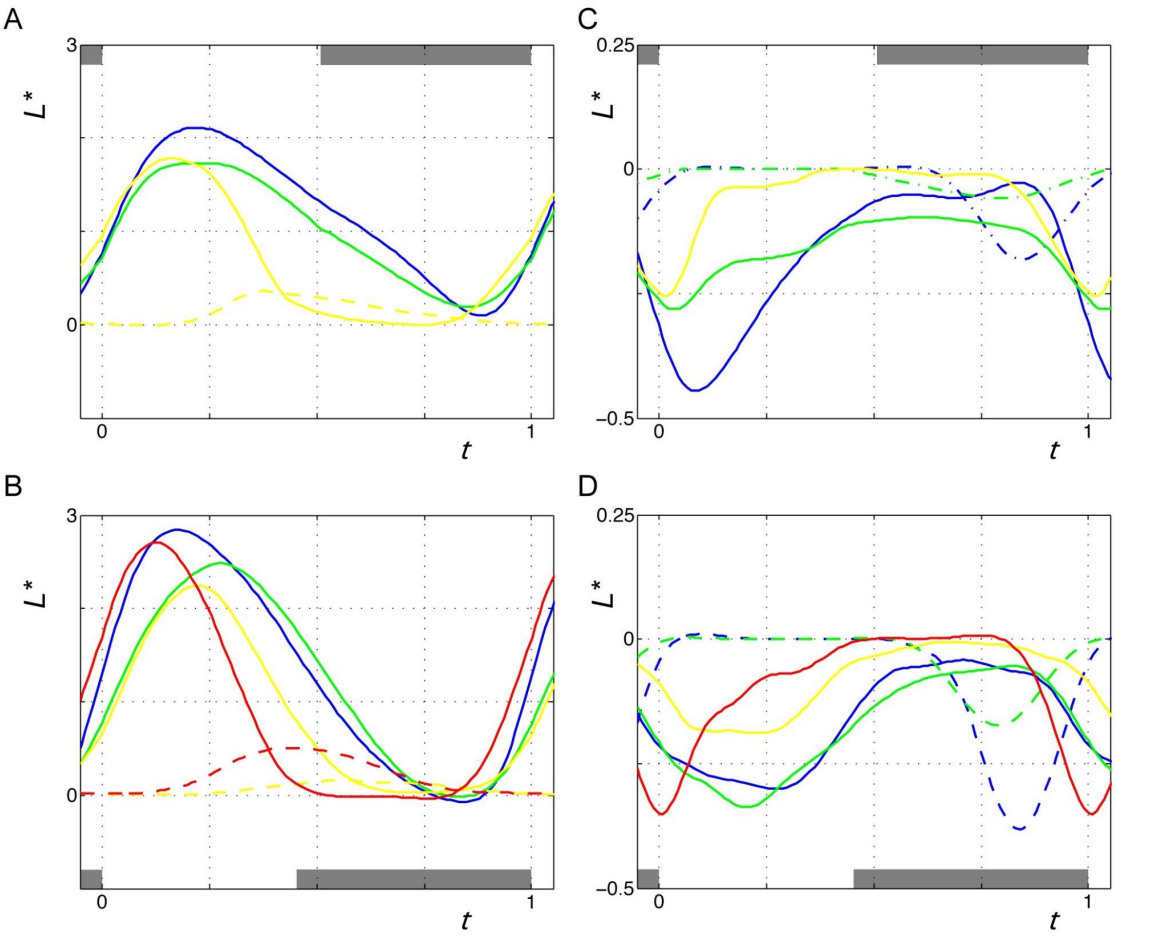

Figure 3. Normalized Lift Throughout the Wingbeat tor the Main Vortex Wake Structures (supplementary Figure S7 in paper). Upper figures are at 4 m/s while lower figures are at 7 m/s. On left, solid lines are from tip vortices and dashed lines are from tail vortices. On right, solid lines are from root vortices and dashed lines on right are from reversed vortex loops. Yellow and red colors are for the two birds species and green and blue are for the two bat species.

References:

Ajanic, E., Feroskhan, M., Mintchev, S., Noca, F., & Floreano, D. (2020). Bioinspired wing and tail morphing extends drone flight capabilities. *Science Robotics*, *5*(47), 1–12. https://doi.org/10.1126/SCIROBOTICS.ABC2897

Chin, D. D., Matloff, L. Y., Stowers, A. K., Tucci, E. R., & Lentink, D. (2017). Inspiration for wing design: How forelimb specialization enables active flight in modern vertebrates. *Journal of the Royal Society Interface*, *14*(131). https://doi.org/10.1098/rsif.2017.0240

Crandell, K. E., & Tobalske, B. W. (2015). Kinematics and aerodynamics of avian upstrokes during slow flight. *Journal of Experimental Biology*, *218*(16), 2518–2527. https://doi.org/10.1242/jeb.116228

Hedenström, A., & Christoffer Johansson, L. (2015). Bat flight: Aerodynamics, kinematics and flight morphology. *Journal of Experimental Biology*, *218*(5), 653–663. https://doi.org/10.1242/jeb.031203

Hedenström, A., Johansson, L. C., & Spedding, G. R. (2009). Bird or bat: Comparing airframe design and flight performance. *Bioinspiration and Biomimetics*, *4*(1). https://doi.org/10.1088/1748-3182/4/1/015001

Hedenström, A., Muijres, F. T., Von Busse, R., Johansson, L. C., Winter, Y., & Spedding, G. R. (2009). High-speed stereo DPIV measurement of wakes of two bat species flying freely in a wind tunnel. *Experiments in Fluids*, *46*(5), 923–932. https://doi.org/10.1007/s00348-009-0634-5

Henningsson, P., & Bomphrey, R. J. (2013). Span efficiency in hawkmoths. *Journal of the Royal Society Interface*, *10*(84), 1–9. https://doi.org/10.1098/rsif.2013.0099

Henningsson, P., & Bomphrey, R. J. (2012). Time-varying span efficiency through the wingbeat of desert locusts. *Journal of the Royal Society Interface*, *9*(71), 1177–1186. https://doi.org/10.1098/rsif.2011.0749

Horstmann, J. T., Henningsson, P., Thomas, A. L. R., & Bomphrey, R. J. (2014). Wake development behind paired wings with tip and root trailing vortices: Consequences for animal flight force estimates. *PLoS ONE*, *9*(3), 1–9. https://doi.org/10.1371/journal.pone.0091040

Hubel, T. Y., Hristov, N. I., Swartz, S. M., & Breuer, K. S. (2016). Wake structure and kinematics in two insectivorous bats. *Philosophical Transactions of the Royal Society B: Biological Sciences*, *371*(1704). https://doi.org/10.1098/rstb.2015.0385

Hubel, T. Y., Hristov, N. I., Swartz, S. M., & Breuer, K. S. (2016). Wake structure and kinematics in two insectivorous bats. *Philosophical Transactions of the Royal Society B: Biological Sciences*, *371*(1704). https://doi.org/10.1098/rstb.2015.0385

Ingersoll, R., Haizmann, L., & Lentink, D. (2018). Biomechanics of hover performance in Neotropical hummingbirds versus bats. *Science Advances*, *4*(9). https://doi.org/10.1126/sciadv.aat2980

James, S., & Cb, C. (1984). *TH E A ER O DY N AM IC S OF H O V E R I N G INSECT F L I G H T . V . A V O R T E X T H E O R Y . 144*, 115–144.

McCracken, G. F., Safi, K., Kunz, T. H., Dechmann, D. K. N., Swartz, S. M., & Wikelski, M. (2016). Airplane tracking documents the fastest flight speeds recorded for bats. *Royal Society Open Science*, *3*(11). https://doi.org/10.1098/rsos.160398

Muijres, F. T., Johansson, L. C., Barfield, R., Wolf, M., Spedding, G. R., & Hedenström, A. (2008). Leading-Edge Vortex Improves Lift in. *Science*, *319*(February), 1250–1253.

Muijres, F. T., Johansson, L. C., Bowlin, M. S., Winter, Y., & Hedenström, A. (2012). Comparing aerodynamic efficiency in birds and bats suggests better flight performance in birds. *PLoS ONE*, *7*(5). https://doi.org/10.1371/journal.pone.0037335

Muijres, F. T., Johansson, L. C., Winter, Y., & Hedenström, A. (2011). Comparative aerodynamic performance of flapping flight in two bat species using time-resolved wake visualization. *Journal of the Royal Society Interface*, *8*(63), 1418–1428. https://doi.org/10.1098/rsif.2011.0015

Muijres, F. T., Spedding, G. R., Winter, Y., & Hedenström, A. (2011). Actuator disk model and span efficiency of flapping flight in bats based on time-resolved PIV measurements. *Experiments in Fluids*, *51*(2), 511–525. https://doi.org/10.1007/s00348-011-1067-5

Sapir, N., Horvitz, N., Dechmann, D. K. N., Fahr, J., & Wikelski, M. (2014). Commuting fruit bats beneficially modulate their flight in relation to wind. *Proceedings of the Royal Society B: Biological Sciences*, *281*(1782). https://doi.org/10.1098/rspb.2014.0018

Spalart, P. R. (2003). On the simple actuator disk. *Journal of Fluid Mechanics*, *494*(494), 399–405. https://doi.org/10.1017/S0022112003006128

Von Busse, R., Hedenström, A., Winter, Y., & Johansson, L. C. (2012). Kinematics and wing shape across flight speed in the bat, Leptonycteris yerbabuenae. *Biology Open*, *1*(12), 1226–1238. https://doi.org/10.1242/bio.20122964